the collapse pressure. In terms of the fluid property, the porosity and permeability are assumed constant as 0.3 and $10^{-12}\,\mathrm{m}^2\cdot\mathrm{sec/Pa}$, respectively. The fluid density is $9.8\,\mathrm{kN/m}^3$ and fluid bulk modulus assumed to be 2.0GPa. For the computation of a tunnel collapse pressure using FLAC^{3D}, we use a stress control method (Mollon et al. 2009). Fig. 4(a) shows the collapse velocity field given by FLAC^{3D}, and Fig. 4(b) shows the corresponding collapse displacement field at the time of failure. Stability against tunnel face collapse is ensured as long as the applied pressure $(\sigma_{applied})$ is greater than the tunnel collapse pressure (σ_T).

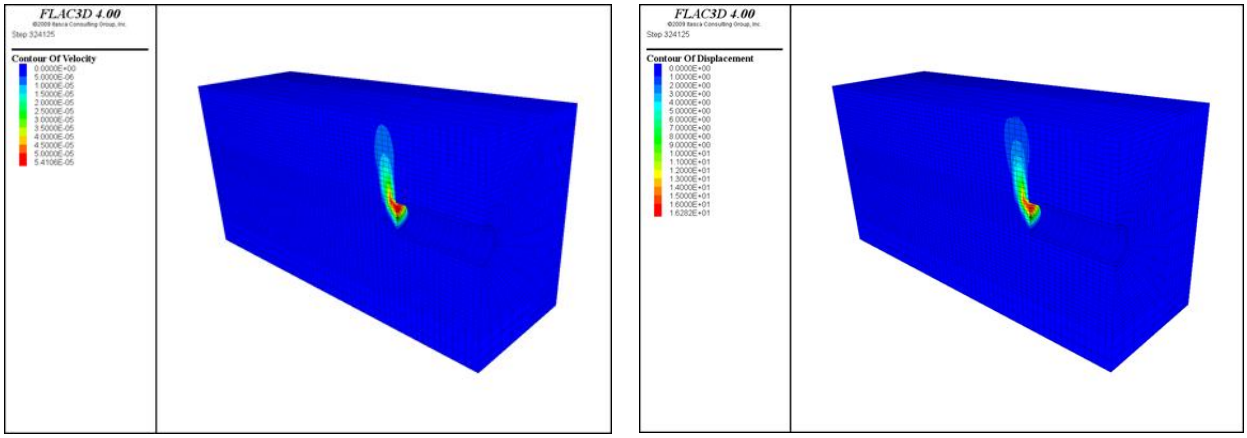

(a) Contour of velocity (b) Contour of displacement

Fig. 4 Calculation of tunnel collapse pressure without seepage

Steady-state flow occurs when at any point in a flow field the magnitude and direction of the flow velocity are constant with time. Transient flow occurs when at any point in a flow field the magnitude or direction of the flow velocity changes with time. The steady-state approach is valid as long as the water table is not drawn down by the existence of the tunnel. Steady-state groundwater flow condition is assumed in the analysis. There are two different types of the drainage condition during a tunnel construction such as the drainage type and the water-proof type. In the drainage type, ground water is drained through the tunnel wall as well as the tunnel face, while in the water-proof type drainage is allowed only through the tunnel face. After applying the hydrostatic heads to the domain as an initial condition, the pressure heads at the wall and the face of the tunnel are taken to be zero in the drainage type while only those of the face are taken to be zero in the water-proof type. During tunnel construction below groundwater level, flow of groundwater into the tunnel leads to total head loss around tunnel, and causes the seepage pressure around the tunnel. Fig. 5(a) and 5(b) show the comparison in the pore pressure distribution between before and after tunnel excavation. Fig. 5(c) and 5(d) show the collapse velocity field with seepage pressure and the corresponding displacement vector at the time of failure. We can see that the location of a failure plane in front of the tunnel face is somewhat changed after the consideration of seepage effect.

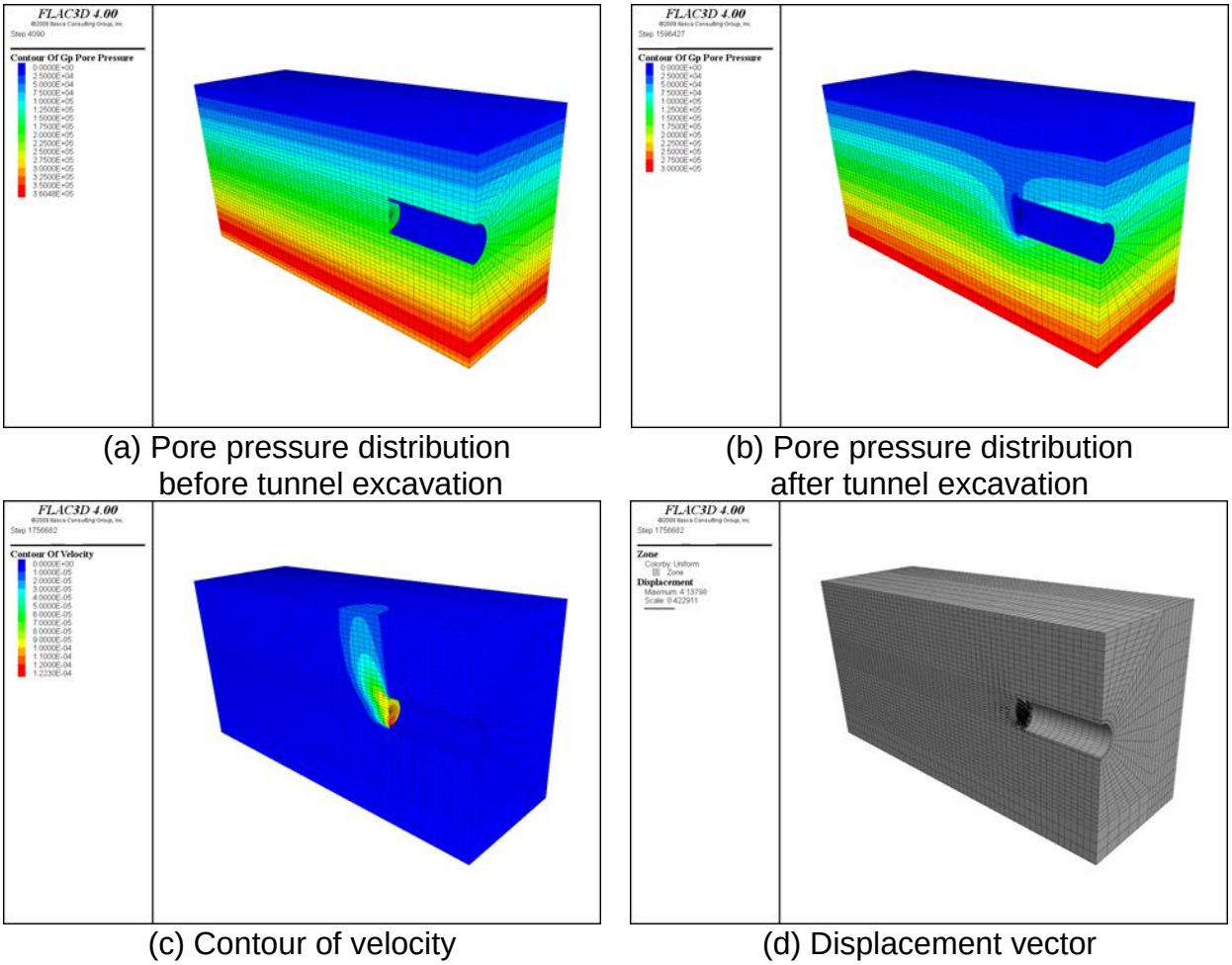

(a) Pore pressure distribution before tunnel excavation

(b) Pore pressure distribution after tunnel excavation

(c) Contour of velocity

(d) Displacement vector

Fig. 5 Calculation of tunnel collapse pressure with seepage

The analyses are conducted for 40 cases of ground conditions as summarized in Table. 1. Each case involves analyses with both the drainage and the water-proof type for the seepage analysis.

3. PROBABILISTIC MODEL FORMULATION

A probabilistic model to predict the limiting collapse pressure of tunnel face can be written as

$$\sigma_T(\mathbf{X}) = \hat{\sigma}_T(\mathbf{X}) + \gamma(\mathbf{X}) + s\varepsilon \tag{10}$$

where, σ_T = the limiting collapse pressure by the FLAC^{3D}, $\hat{\sigma}_T$ = the limiting collapse pressure by the upper bound theorem is defined in Eq. (1),

$\mathbf{X} = (\alpha, \beta, k_1, k_2, c_0', \phi', \rho, \gamma, C, D, \sigma_S, \sigma_{S.F.}) =$ the random variables, $\gamma(\mathbf{X}) =$ the correction term for the bias inherent in the deterministic model that is expressed as a function of the variables $\mathbf{X}$, $s\varepsilon =$ the model error, $s =$ the unknown standard deviation of the model error, $\varepsilon =$ a random variable with zero mean and unit variance of standard normal distribution. In assessing the probabilistic model, the following assumptions are made: (a) the model variance σ^2 is independent of $\mathbf{X}$ (homoskedasticity assumption), and (b) ε follows the normal distribution (normality assumption). These assumptions are verified by using diagnostic plots of the data or the residuals versus the model predictions. After reviewing the diagnostic plot of the residuals as shown in Fig. 6(a), we introduce the constant correction term that is independent of the random variables, $\gamma(\mathbf{X}) =$ 0.075, to remove potential bias in the model. The normality assumption is also checked in the Q-Q normal plot of the residuals as shown in Fig. 6(b). Fig. 7 shows the comparison in the limiting collapse pressure between by UBM solutions and FLAC^{3D} numerical models.

Table 1. Cases of analysis for the calculation of the limiting collapse pressure

		c_0'									
		0	0.25	0.50	0.75	1.00	1.25	1.50	2.00	2.50	3.00
ρ	0	Case M01	Case M02	Case M03	Case M04	Case M05	Case M06	Case M07	Case M08	Case M09	Case M10
	1.00	Case M11	Case M12	Case M13	Case M14	Case M15	Case M16	Case M17	Case M18	Case M19	Case M20
	1.50	Case M21	Case M22	Case M23	Case M24	Case M25	Case M26	Case M27	Case M28	Case M29	Case M30
	2.00	Case M31	Case M32	Case M33	Case M34	Case M35	Case M36	Case M37	Case M38	Case M39	Case M40

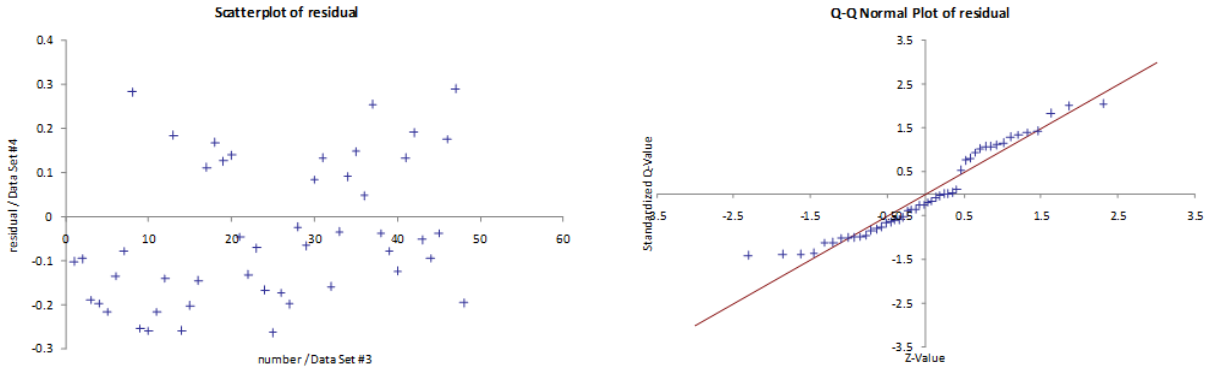

(a) Diagnostic plot (b) Q-Q normal plot

Fig. 6 Residual analysis

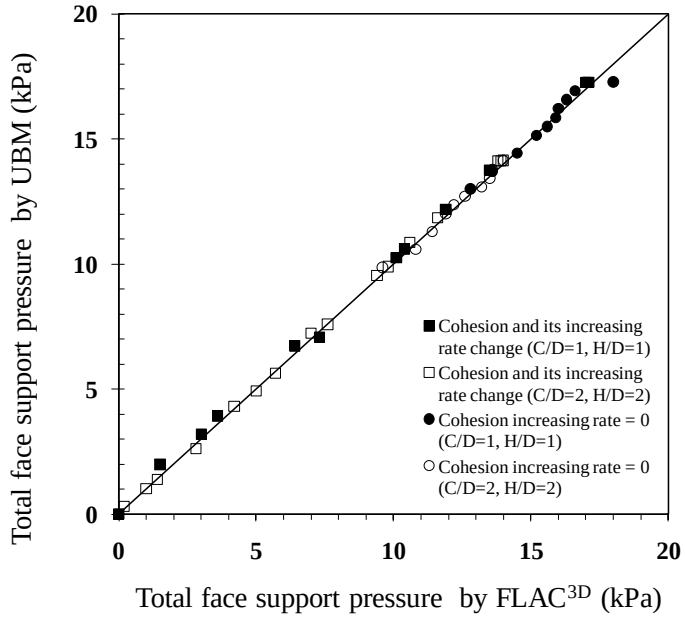

Fig. 7 Comparison in the limiting collapse pressure between UBM and FLAC^{3D} numerical models

4. RELIABILITY ANALYSIS

The limit state function, $g(\mathbf{X})$, with respect to the collapse of tunnel face in the ultimate limit state (ULS) can be described as

$$g(\mathbf{X}) = \sigma_{applied} - \sigma_T(\mathbf{X}) \tag{11}$$

where, $\sigma_{applied} =$ the applied pressure on the tunnel face and $\sigma_T(\mathbf{X}) =$ the limiting collapse pressure calculated by the FLAC^{3D} as described in the previous section.

When a probabilistic stability analysis is conducted, the failure probability for the tunnel face collapse can be defined as:

$$p_f = P\left[g(\mathbf{X}) \le 0\right] = \int_{g(\mathbf{X})\le 0} f(\mathbf{X}) d\mathbf{X} \tag{12}$$

where $f(\mathbf{X})$ is the joint probability density function of the basic variable vectors $\mathbf{X} = (\alpha,\ \beta,\ k_1,\ k_2,\ c_0',\ \phi',\ \rho,\ \gamma,\ C,\ D,\ \sigma_S,\ \sigma_{S.F.})$. The reliability analyses using first-order reliability method (FORM), the second-order reliability method (SORM), and Monte Carlo simulations (MCS) are performed based on the parameters summarized in

Table 2. In this case, some of the parameters (C, D, σ_S, $\sigma_{S.F.}$) are assumed to be constant values.

Table 2. Parameters for the reliability analysis

Parameter ranges	Distribution models	Mean	COV
$0 < c_0' < \infty$	Lognormal	1.00	0.20
$0 < \phi' < \infty$	Lognormal	35.0	0.20
$0 < \rho < \infty$	Lognormal	0.50	0.20
$0 < \gamma < \infty$	Lognormal	15.2	0.20
C=10.0m, D=5.0m, σ_S=10kN/m^2, $\sigma_{S.F.}$=34.9kN/m^2			

The reliability index for the different applied pressure values can be obtained as shown in Fig. 8. As the applied pressure on the tunnel face increase, the reliability index also increases and it also means that the probability of failure will decrease.

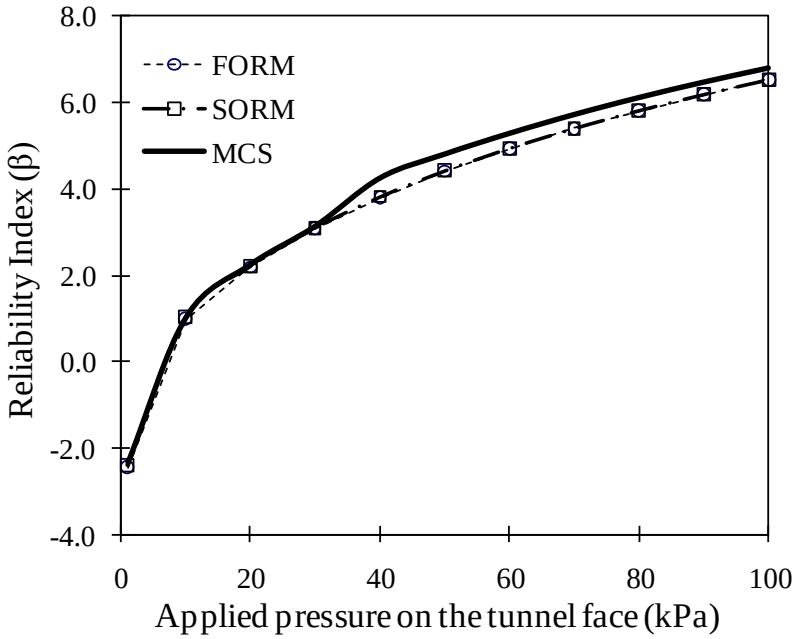

Fig. 8 Reliability index for the different applied pressure values

5. SENSITIVITY AND IMPORTANCE MEASURES

In a reliability analysis, sensitivity measures are used to determine the effects on the reliability of changes in the parameters in the limit state function or in the distribution of the random variables. Fig. 9 shows the sensitivity measures as a function of the applied pressure on the tunnel face. It is observed that ϕ' have larger effects on

the reliability. As the applied pressure increases, the tunnel face stability is most sensitive to ϕ'. Fig. 10 shows the importance measures of all random variables for the tunnel face stability. Observations similar to those made for the sensitivity analysis can be made for the importance measures. We can see that ϕ' is the most important variable and γ is the second most important variable.

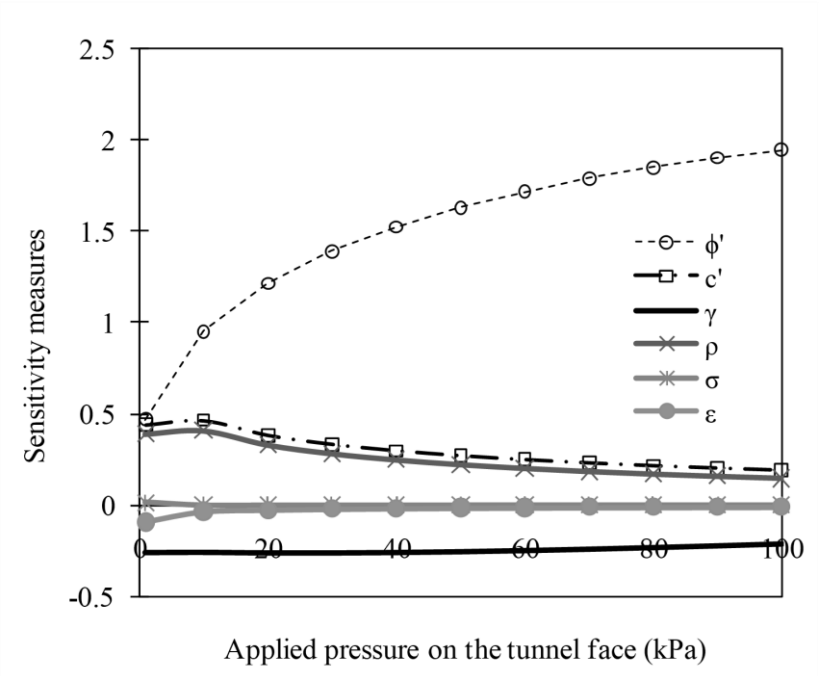

Fig. 9 Sensitivity measures for the random variables

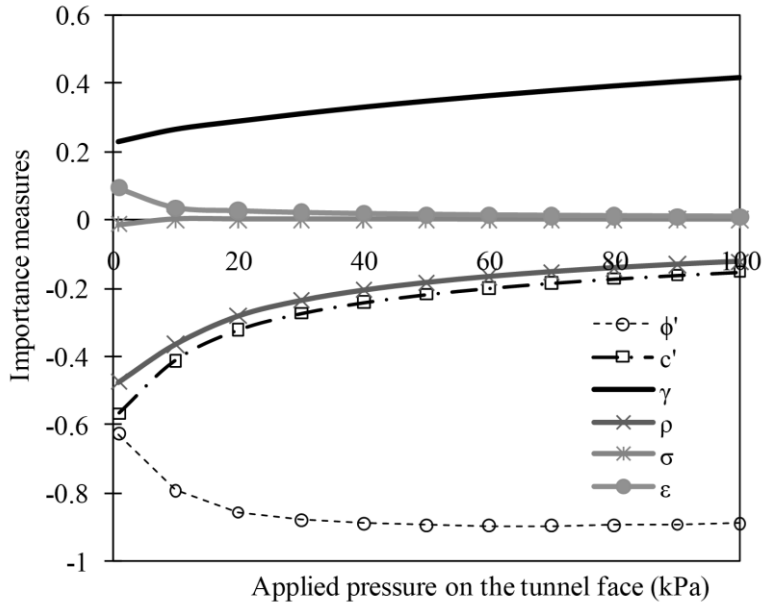

Fig. 10 Importance measures for the random variables

6. CONCLUSIONS

The limiting tunnel collapse pressure in a Mohr-Coulomb (c', ϕ') soil from the upper bound method (UBM) of limit analysis theory which can consider the effect of seepage into the tunnel face and strength increase with depth. The influence of seepage forces and depth-dependent effective cohesion is investigated for a dual-cone failure mechanism using the UBM implemented by numerical analysis. The upper bound analytical derivation for depth-dependent effective cohesion and corresponding numerical results are presented and compared to those presented by previous authors. In addition, the numerical analysis demonstrated the influence of tunnel diameter on required face supporting pressure.

After the UBM solution is verified with the numerical experiments, the probabilistic model is proposed to calculate the unbiased limiting tunnel collapse pressure. A reliability analysis of a shallow circular tunnel driven by a pressurized shield in a frictional and cohesive soil is presented to consider the inherent uncertainty in the input parameters and the proposed model. The ultimate limit state (ULS) for the face stability is considered in the analysis. The probability of failure that exceeding a specified applied pressure at the tunnel face is estimated. Sensitivity and importance measures are computed to identify the key parameters and random variables in the model.

REFERENCES

Atkinson, J. H., and Potts, D. M. (1977). "Stability of a shallow circular tunnel in cohesionless soil." *Géotechnique*, **27**(2), 203-215.

Chambon, P., and Corte, J.-F. (1994). "Shallow tunnels in cohesionless soil: Stability of tunnel face." *Journal of Geotechnical Engineering*, **120**(7), 1148-1165.

Davis, E. H., Gunn, M. J., Mair, R. J., and Seneviratne, H. N. (1980). "The stability of shallow tunnels and underground openings in cohesive material." *Géotechnique*, **30**(4), 397-416.

Eclaircy-Caudron, S., Dias, D., and Kastner, R. (2007). "Assessment of soil parameters met during a tunnel excavation: Use of inverse analysis on in situ measurements---Case of Bois de Peu (France)." *Advances in Measurement and Modeling of Soil Behavior (GSP 173)*, ASCE, Denver, CO, 1-10.

FLAC^{3D}. (2009). *Fast Lagrangian Analysis of Continua in 3 Dimensions*. ITASCA Consulting Group, Inc., Minneapolis, Minnesota.

Jardine, R. J., Potts, D. M., Fourie, A. B., and Burland, J. B. (1986). "Studies of the influence of non-linear stress strain characteristics in soil-structure interaction." *Géotechnique*, **36**(3), 377-396.

Leca, E., and Dormieux, L. (1990). "Upper and lower bound solutions for the face stability of shallow circular tunnels in frictional material." *Géotechnique*, **40**(4), 581-606.

Mollon, G., Dias, D., and Soubra, A.-H. (2009). "Probabilistic analysis of circular tunnels in homogeneous soil using response surface methodology." *Journal of Geotechnical and Geoenvironmental Engineering*, **135**(9), 1314-1325.

Mroueh, H., and Shahrour, I. (2003). "A full 3-D finite element analysis of tunneling-adjacent structures interaction." *Computers and Geotechnics*, **30**(3), 245-253.

Park, J. K. (2011). Adaptive Reliability Analysis of Excavation Problems. Doctoral dissertation, Texas A&M University.

Wong, H., Subrin, D., and Dias, D. (2006). "Convergence-confinement analysis of a bolt-supported tunnel using the homogenization method." *Canadian Geotechnical Journal*, **43**(5), 462-483.

Yoo, C. (2002). "Finite-element analysis of tunnel face reinforced by longitudinal pipes." *Computers and Geotechnics*, **29**(1), 73-94.